IRON LINES IN THE SPECTRA OF X-RAY BINARIES

M. M. Basko

Space Research Institute
Academy of Sciences of the USSR
Moscow 117810 USSR

INTRODUCTION

The discovery of an iron line emission at $\epsilon = 6$–7 keV is the first prominent achievement of cosmic x-ray spectroscopy. Now this line is found in the spectra of almost all types of cosmic x-ray sources, including x-ray binaries,[1-7] supernova remnants,[8-11] single galaxies,[12] and clusters.[13-15] For many of them a theoretical interpretation of the iron line emission presents no difficulty. In the case of supernova remnants and clusters of galaxies the x-ray flux both in lines and continua comes as a thermal emission of hot ($T > 10^7$ K) optically thin gas clouds—a model thoroughly explored by theoreticians. The line is excited by electron collisions with Fe^{+25} and Fe^{+25} ions. A different mechanism operates in the active galaxy Cen A, where the iron line emission is due to K_α fluorescence of a cold ($T < 10^7$ K) gas surrounding the central x-ray source with a continuous spectrum. Here the excitation mechanism is the K-shell photoionization of low ions of iron Fe I–XVII. Such a model is characterized by a specific relation between the K_α-line ($\epsilon = 6.40$ keV) equivalent width and the magnitude of the K jump at $\epsilon = 7.11$ keV : the number of line photons emitted is three times less (the fluorescence yield $\omega_K = 0.34$) than the number of photons absorbed in the continuum above the K edge.

In the case of x-ray binaries, however, the attempts to explain the observed properties of iron line emission meet with serious difficulties. I shall try to illustrate this with an example of the best studied x-ray binary Her X-1. We know that the x-ray spectrum of this source is formed in hot regions at the magnetic poles, where the accreting material collides with the surface of the neutron star. If one assumes that the hot spots occupy $\sim 1/100$ of the total surface area of the neutron star (a typical value in the theory of x-ray pulsars), then the photoionization rate for Fe^{+25} in the atmosphere is $\gamma^{+25} \approx 7.3 \times 10^{12} L_{37}\ s^{-1}$, where L_{37} is the x-ray luminosity in units of 10^{37} erg s^{-1}. From the shape of the x-ray spectrum of Her X-1 one can say that the electron temperature in the atmosphere of hot spots $T \gtrsim 10^8$ K, and the scale height is $H \approx 10^2$ cm. The recombination coefficient at such a temperature is $\alpha_{tot}{}^{+25} \approx 1.3 \times 10^{-12}$ cm^3 s^{-1}, and for the electron density $n_e = (\delta_T H)^{-1} \approx 1.5 \times 10^{22}$cm^{-3} at the level with Thomson optical depth $\tau_T = 1$ we arrive at the value of Fe^{+25} concentration $\chi^{+25} \approx 10^{-3}$. Under these conditions the principal mechanism of populating the $2p$ level of Fe^{+25} is recombination, and according to Equations 9 and 10a (in Equation 9 one must set $\Omega_s = 4\pi/100$, $r_A = R \approx 10^6$ cm, $\tau_T = 1$) the equivalent width of the iron line $W \approx 1$ eV, if one assumes normal chemical composition. The above value of W is at least two orders of magnitude less than the observed one, $W \approx 300$ eV.[3] Mészáros[16] obtained similar values, $W < 10$ eV, in the case of disk accretion onto black holes.

Thus, a natural suggestion comes to mind that in x-ray binaries the iron line is formed away from the x-ray star, and the excitation is due to fluorescence. A

0077-8923/80/0336-0566 $01.75/1 © 1980, NYAS

fluorescent K_α line of iron, originating in the atmosphere of the normal component of the binary, had been predicted[17] more than four years ago. The detailed calculations[18,19] have shown, however, that this line is not what is observed because it should (i) have significantly smaller values of the equivalent width ($W \approx 15$ eV for Her X-1); (ii) show strong correlation with the orbital phase, which contradicts the observations of Her X-1[3] and Cyg X-3[6]; (iii) be centered at $\epsilon = 6.40$ keV and have a small width $\Delta\epsilon \sim 30$ eV, which is in a disagreement with reference 7.

And even when one adds the fluorescence of the accretion disk and that of the stellar wind, the theoretical values of W for the HZ Her /Her X-1 system[19] are still 3–5 times less than the observed ones.

But though K_α fluorescence of weakly ionized iron fails to account for the observed emission feature, I should like to emphasize that the narrow K_α line *has to be found* in the spectra of x-ray binaries at the level predicted by the above mentioned calculations[18,19] (if our understanding of these objects is any good). The discovery and systematic observations of this line will render us much new information about that type of cosmic x-ray source. Possibly, it is this line that has been detected[20] in the "off" state of Her X-1.

Below I shall consider a model that is an attempt to explain the observed powerful iron line emission as a fluorescence of the gaseous shell at the Alfvén surface. It has been realized recently, when trying to interpret the observed pulse profile and soft x-ray emission of Her X-1,[21–23] that the Alfvén shell may be an important constituent of the models of binary x-ray pulsars. Calculations of the iron line emission presented below give some more support to this idea. In my opinion, the model under discussion is the only one for the time being that can claim to be able to account for the observed properties of the iron line in x-ray binaries, but it has its difficulties too.

Parameters of the Gas in the Alfvén Shell

The location of the Alfvén shell r_A to a great extent depends on the accretion geometry in the region $r > r_A$. In a spherically symmetric case[24–26]

$$r_A \gtrsim r_A^0 = 2^{-3/7}\mu^{4/7}(LR)^{-2/7}(GM)^{1/7}$$
$$= 2.89 \times 10^8\, \mu_{30}^{4/7}(L_{37}R_6)^{-2/7}(M/M_\odot)^{1/7}\ \text{cm}, \qquad (1)$$

where μ_{30} is the dipole magnetic moment of the neutron star in units of 10^{30} G cm^3, M is its mass, R_6 is its radius in units of 10^6 cm, and L_{37} is the x-ray luminosity in units of 10^{37} erg s^{-1}. In the case of disk accretion the radius of the Alfvén shell is much more uncertain, although the theoretical estimates[27,28] show it to be of the same order of magnitude as r_A^0. Keeping in mind this uncertainty and the fact that the HZ Her/Her X-1 system disk accretion takes place, I shall treat r_A as *a free parameter* that is to be determined from comparison of the observed value of the iron line equivalent width with the calculated one.

It will be only natural to assume that the Alfvén shell subtends a substantial solid angle $\Omega_s \gtrsim 1$ as seen from the neutron star, since otherwise its contribution to the iron line emission will not be dominating. But in order for the accreting material to come out of the disk plane and spread along the magnetic field lines over a substantial solid

TABLE 1

THE VALUES OF PHYSICAL PARAMETERS IN THE ALFVÉN SHELL AND THE EQUIVALENT WIDTH OF THE IRON LINE FOR $\mu = 10^{30}$ G cm^3

R_A (cm)	10^8	7×10^7	5×10^7	4×10^7	3×10^7	2.5×10^7	2.34×10^7	2×10^7
ξ	3.53×10^4	1.21×10^4	4.41×10^3	2.26×10^3	953	552	458	282
n_e(cm^{-3})	8.50×10^{16}	5.06×10^{17}	2.72×10^{18}	8.30×10^{18}	3.50×10^{19}	8.70×10^{19}	1.19×10^{20}	2.66×10^{20}
T(K)	4.01×10^7	2.83×10^7	1.33×10^7	6.79×10^6	2.82×10^6	1.60×10^6	1.34×10^6	1.52×10^6
x^{+25}	0.0118	0.04426	0.1835	0.3817	0.4023	0.2402	0.1908	0.1387
x^{+24}	4.57×10^{-5}	6.75×10^{-4}	0.01432	0.09868	0.4729	0.7305	0.7920	0.8529
x^{+7}	3.44×10^{-5}	1.33×10^{-4}	7.29×10^{-4}	2.71×10^{-3}	1.43×10^{-2}	3.83×10^{-2}	5.22×10^{-2}	7.46×10^{-2}
W^{+25}(eV)	0.49	2.3	12.6	32	43	29	24	19
W^{+24}(eV)	5.2×10^{-3}	0.095	2.5	21	125	217	245	285
$\tau_{ff}\|_{\epsilon=kT}$	4.9×10^{-9}	1.2×10^{-7}	1.0×10^{-5}	3.8×10^{-4}	0.040	0.79	2.1	3.2
L_π/L	7.0×10^{-4}	2.0×10^{-3}	4.6×10^{-3}	7.1×10^{-3}	1.3×10^{-2}	1.8×10^{-2}	2.0×10^{-2}	2.4×10^{-2}

angle, the condition

$$\rho v^2 \leq H^2/8\pi \tag{2}$$

must be fulfilled in the Alfvén shell. And since from the very meaning of the Alfvén surface the strong inequality cannot obtain in (2), we can use Equation 2 to estimate the electron density in the shell. The calculations of the gas flow in the Alfvén shell[26] show that over the major part of the shell one can, with a sufficient degree of accuracy, adopt $V \approx 0.3V_{ff} = 0.3\,(2GM/r_A)^{1/2}$. Assuming $N_{He} = 0.1\,N_H$, from (2) we get

$$N_e = 8.5 \times 10^{16}\,\mu_{30}^{\,2}\,r_8^{\,-5}\,(M/M_\odot)^{-1}\ \mathrm{cm}^{-3}. \tag{3}$$

Here r_8 is the Alfvén radius r_A in units of 10^8cm.

The Thomson optical depth $\tau_T = \sigma_T N_e \delta$ of the shell can be estimated from the condition that all material falling into the neutron star, $\dot{M} = LR/GM$, passes through the cross section $S \approx \Omega_s r_A \delta$ of the shell,

$$\tau_T = 0.52\,L_{37}\,r_8^{\,-1/2}\,\Omega_s^{\,-1}\,R_6\,(M/M_\odot)^{-3/2}. \tag{4}$$

The formula (4) is valid for $\delta \ll r_A$, which is equivalent to the condition $r_A < (\Omega_s/3.8)^{2/7} r_A^{\,0}$ that always holds in cases of interest here.

All estimates below are performed for Her X-1, for which within a factor $\lesssim 2$, $L_{37} = 3$, $R_6 = M/M_\odot = 1$, and $\Omega_s = 3$. The value of the dipole magnetic moment is much more uncertain, and the calculations were done for $\mu_{30} = 1$ (TABLE 1) and $\mu_{30} = 10$ (TABLE 2).

THERMAL BALANCE AND IONIZATION EQUILIBRIUM

Since according to Equation 4 the Thomson optical depth of the shell $\tau_T \lesssim 1$, the temperature and the ionization balance can be evaluated in the optically thin approximation. In this approximation they depend (for a fixed x-ray spectrum) on one parameter only,

$$\xi = L/n_e r_A^{\,2} = 1.18 \times 10^4\,L_{37}\,\mu_{30}^{\,-2}\,r_8^{\,3}\,(M/M_\odot). \tag{5}$$

In the range of interest here, $\xi > 10^2$, it is sufficient to include in the equation of thermal balance the following processes:[29] Compton heating, bremsstrahlung cooling, heating and cooling by photoionization, and recombination of oxygen ($O^{+8} \rightleftarrows O^{+7}$) and iron ($Fe^{+26} \rightleftarrows Fe^{+25} \leftrightarrows Fe^{+24}$) ions. The cooling in the resonance line of He^+ can be neglected here because the values of $\xi \lesssim 300$, at which it might become important, are attained at such a high density in the shell that the electron deexcitation of the $2p$ level of He^+ completely dominates its radiative decay, while the optical depth in the line $\tau \gtrsim 10^3$. Under such conditions only a small fraction of L_α photons of He^+ created in the shell escapes.

If such a high density is adopted in the shell that it becomes opaque for the photons $\epsilon \sim kT$, the free–free cooling occurs through the surface emission rather than through the emission out of the whole volume. For more details on thermal balance see reference 30. The plot of the temperature $T(\xi)$ evaluated as described above is shown in FIGURE 1.

TABLE 2

THE VALUES OF PHYSICAL PARAMETERS IN THE ALFVÉN SHELL AND THE EQUIVALENT WIDTH OF THE IRON LINE FOR $\gamma = 10^{31}$ G cm^3

R_A(cm)	4×10^8	3×10^8	2.5×10^8	2×10^8	1.5×10^8	1.0×10^8	8.24×10^7	7.5×10^7
ξ	2.26×10^4	9.53×10^3	5.52×10^3	2.82×10^3	1.19×10^3	353	197	149
n_e(cm^{-3})	8.30×10^{15}	3.50×10^{16}	8.70×10^{16}	2.66×10^{17}	1.12×10^{18}	8.50×10^{18}	2.24×10^{19}	3.58×10^{19}
T(K)	3.61×10^7	2.47×10^7	1.64×10^7	8.52×10^6	3.56×10^6	1.06×10^6	6.98×10^5	7.57×10^5
x^{+25}	0.0200	0.0615	0.134	0.134	0.445	0.136	0.0624	0.0504
x^{+24}	1.32×10^{-4}	1.34×10^{-3}	7.09×10^{-3}	0.0546	0.353	0.856	0.936	0.949
x^{+7}	5.82×10^{-5}	1.90×10^{-4}	4.80×10^{-4}	1.75×10^{-3}	9.35×10^{-3}	0.0783	0.171	0.205
W^{+25}(eV)	0.42	1.58	4.0	11.5	20.6	8.5	4.44	3.74
W^{+24}(eV)	7.6×10^{-3}	0.092	0.56	5.1	41	130	159	168
$\tau_{ff}\|_{\epsilon=kT}$	3.46×10^{-10}	6.31×10^{-9}	7.27×10^{-8}	2.44×10^{-6}	2.54×10^{-4}	0.163	2.04	2.58
L_{ff}/L	5.19×10^{-4}	1.18×10^{-3}	1.81×10^{-3}	2.85×10^{-3}	5.04×10^{-3}	1.14×10^{-2}	1.82×10^{-2}	2.09×10^{-2}

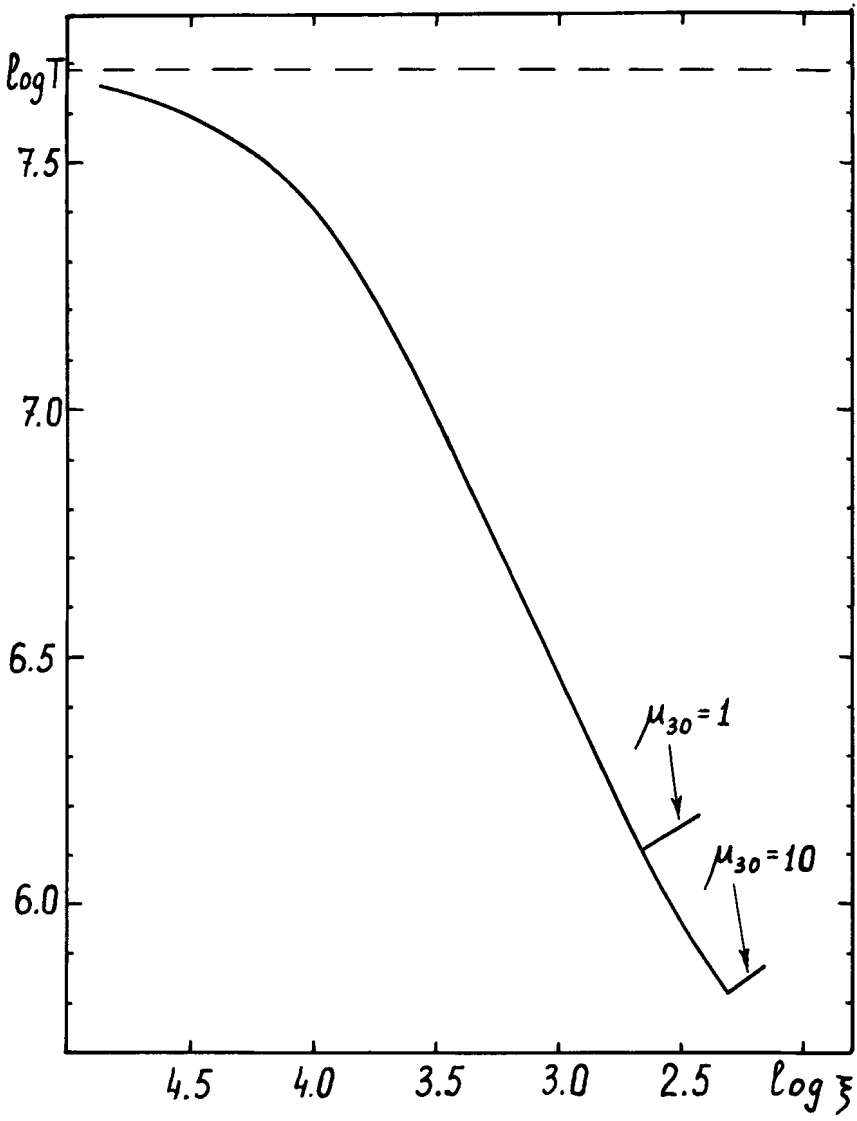

FIGURE 1. The electron temperature T in the Alfvén shell as a function of parameter $\xi = L/n_e r_A^2$.

The ionization equilibrium was calculated according to the following equations:

$$\gamma^{+25} x^{+25} = \alpha_{\text{tot}}{}^{+25} n_e (1 - x^{+25} - x^{+24}), \tag{6a}$$

$$\gamma^{+24} x^{+24} = \alpha_{\text{tot}}{}^{+24} n_e x^{+25}, \tag{6b}$$

$$(\gamma^{+7} + C^{+7} n_e) x^{+7} = \alpha_{\text{tot}}{}^{+7} n_e (1 - x^{+7}), \tag{7}$$

where x^{+24}, x^{+25}, and x^{+7} are the fractions of ions Fe^{+24}, Fe^{+25}, and O^{+7}; γ^{+n} is the rate of photoionization by x-rays of the corresponding ion; $\alpha_{tot}{}^{+n}$ is the recombination coefficient summed over all excited levels; C^{+7} is the electron impact ionization coefficient for the ion O^{+7}. The contributions of electron impact ionization of iron, of dielectronic recombination onto Fe^{+25}, and of triple recombination can be safely neglected under the conditions of interest here.

I do not include in the present calculations the low stages of ionization of the iron atoms Fe^{+23}, Fe^{+22}, ..., which make a significant contribution at $\xi \lesssim 500$. This neglect, however, has only a slight effect on the total equivalent width $W = W^{+25} + W^{+24}$ of the line, because it does not change appreciably the total number of K-shell ionizations.

Equivalent Width of the Iron Line

A posteriori one can easily verify that the principal mechanism of populating the level $n = 2$ in ions Fe^{+25} and Fe^{+24} in the Alfvén shell is cascading by recombination.* The relative contribution of the electron impact excitation never exceeds 1%. And since the shell is opaque in lines formed by direct transitions from levels $n \geq 3$ to the ground state,[30] one can think of each electron recombining to any excited level $n > 2$ of Fe^{+25} and Fe^{+24} as coming down ultimately to the level $n = 2$. Of all ways by which the radiative decay of the level $n = 2$ can occur, only the four most probable are of practical interest: $2P_{3/2} \rightarrow 1S_{1/2}$ and $2P_{1/2} \rightarrow 1S_{1/2}$ in Fe^{+25} (photon energies $\epsilon = 6.97$ keV and $\epsilon = 6.95$ keV), and $2^1P_1 \rightarrow 1\ S_0$ and $2^3P_1 \rightarrow 1^1S_0$ in Fe^{+24} (photon energies $\epsilon = 6.70$ keV and $\epsilon = 6.67$ keV). All other radiative transitions are quenched by collisions with charged particles, if only $n_e \gtrsim 10^{18}\text{cm}^{-3}$.[30] Having assumed that the population rates of the $2P_{1/2}$ and $2P_{3/2}$ levels in Fe^{+25}—as well as of singlet and triplet levels in Fe^{+24}—are proportional to their statistical weights, we obtain the following relationships for the line intensities:

$$I(1S_{1/2} - 2P_{1/2}) : I(1S_{1/2} - 2P_{3/2}) = 1{:}2, \tag{8a}$$

$$I(1^1S_0 - 2^1P_1) : I(1^1S_0 - 2^3P_1) = 1{:}3. \tag{8b}$$

In view of Equations 8, the total line intensities for each of the two ions Fe^{+24} and Fe^{+24} will be given below.

The equivalent width of the iron line emitted by the Alfvén shell is

$$W = \beta n_{Fe} \frac{\tau_T}{\sigma_T} \frac{\epsilon_0 \epsilon_{max}}{L} \Omega_s r_A{}^2 =$$

$$= 6.85 \times 10^{11}\, \beta \tau_T L_{37}{}^{-1} \mu_{30}{}^2 r_8{}^{-3} \Omega_s (M/M_\odot)^{-1} Y_{Fe}\ \text{eV}, \tag{9}$$

where the excitation coefficient $\beta(\text{cm}^3\,\text{s}^{-1})$ is given by

$$\beta^{+25} = (\alpha_{tot}{}^{+25} - \alpha_1{}^{+25})(1 - x^{+25} - x^{+24}), \tag{10a}$$

$$\beta^{+24} = (\alpha_{tot}{}^{+24} - \alpha_1{}^{+24})\, x^{+25}. \tag{10b}$$

*When combined with the fact that iron is ionized exclusively by the x-ray continuum from the central source, this justifies the use of the term "fluorescence" for the line emission mechanism under discussion.

In deriving Equation 9, it is taken into account that all the line photons $\epsilon_0 = 6.7$ keV escape from the shell,[30] and the spectrum of the central x-ray source is assumed to be flat, $dL/d\epsilon$ = constant, up to the photon energy $\epsilon_{max} = 20$ keV. The iron abundance is written in the form

$$n_{Fe} = 3 \times 10^{-5} n_H Y_{Fe}. \tag{11}$$

Inserting τ_T from Equation 4 into Equation 9, we get

$$W = 3.56 \times 10^{11} \beta \mu_{30}^2 r_8^{-7/2} R_6 (M/M_\odot)^{-5/2} Y_{Fe} \text{ eV}. \tag{12}$$

It is difficult to judge the dependence of W on the Alfvén radius r_A and other parameters of the neutron star by appearance of Equation 12 since a complicated function β enters there. This dependence can be easily examined, however, in two limiting cases: (i) the iron is almost fully ionized, $x^{+24} \ll x^{+25} \ll 1$, which occurs at radii $r_A \gtrsim 0.2\, r_A^0$ where $T \gtrsim 10^7$ K; (ii) the iron is predominantly in the form of ions with the filled K shell, $x^{+25} \ll 1$, $1 - x^{+24} \ll 1$, which occurs at radii $r_A \lesssim 0.1\, r_A^0$ where $T \sim 10^{6K}$. When we note that $W^{+25} \gg W^{+24}$ in case (i), and $W^{+24} \gg W^{+25}$ in case (ii), and make necessary simplifications in Equations 12 and 10 with the aid of Equation 6b, we get

$$W \approx \begin{cases} 3.56 \times 10^{11} (\alpha_{tot}^{+25} - \alpha_1^{+25}) \mu_{30}^2 r_8^{-7/2} R_6 (M/M_\odot)^{-5/2} Y_{Fe} \text{ eV}, & r_A \gtrsim 0.2\, r_A^0, \quad \textbf{(13a)} \\ 62.8\, (1 - \alpha_1^{+24}/\alpha_{tot}^{+24}) L_{37} z_8^{-1/2} R_6 (M/M_\odot)^{-3/2} Y_{Fe} \text{ eV}, & r_A \lesssim 0.1\, r_A^0. \quad \textbf{(13b)} \end{cases}$$

From Equation 13a one sees that while $r_A \gtrsim 0.2 r_A^0$, the equivalent width of the iron line rapidly increases with the decreasing r_A—more rapidly than $r_A^{-7/2}$ because the decrease of r_A is accompanied with the increase in recombination rate $(\alpha_{tot}^{+25} - \alpha_1^{+25})$ due to the temperature drop. Nevertheless, the typical values of $W \lesssim 10$ eV in this region. At still lower values of $r_A \lesssim 0.1\, R_A^0$ the dependence $W(r_A)$ flattens and becomes so weak, $W \propto r_A^{-1/2}$, that one can consider the value $W_{max} = W(0.1\, r_A^0)$ given by Equation 13b as *the maximum possible value of the iron line equivalent width that can be expected from the Alfvén shell* (a weak dependence of the factor $(1 - \alpha_1^{+24}/\alpha_{tot}^{+24})$ on the temperature T is unimportant for $T \lesssim 3 \times 10^6$ K). From Equation 13b it follows that W_{max} is directly proportional to the luminosity L of the x-ray source, and increases with the increasing hardness of its spectrum, namely

$$W_{max} \propto \int_{\epsilon_{th}}^{\infty} \frac{dL}{d\epsilon} \left(\frac{\epsilon_{th}}{\epsilon}\right)^{2.84} \frac{d\epsilon}{\epsilon}, \tag{14}$$

where $\epsilon_{th} = 8.83$ keV is the ionization threshold of Fe^{+24}. The typical values of W_{max} amount to a few hundreds of electron volts—just what is observed. It is interesting to note that W_{max} does not depend on the magnetic moment μ (as long as $r_A > R$). It should be mentioned also that W is always proportional to the iron abundance Y_{Fe}, and does not depend on the value of the solid angle Ω_s until the optically thin approximation breaks down.

The values of equivalent widths W^{+25} and W^{+24}, calculated separately for ions Fe^{+25} and Fe^{+24}, are listed in TABLES 1 ($\mu_{30} = 1$) and 2 ($\mu_{30} = 10$). These tables contain

also such other parameters of the shell as plasma temperature and density, fractions of iron and oxygen ions, free–free optical depth at the frequency $\epsilon = kT$, ratio of soft to hard x-ray luminosities L_{ff}/L and parameter ξ.

The Profile of the Iron Line

Locally, at each point of the Alfvén shell every component of the iron line originating from a particular atomic transition is rather narrow. The Doppler broadening (which exceeds the natural width) is small enough,

$$\Delta\epsilon_D = \epsilon(2kT/Am_pC^2)^{1/2} = 0.4T_6^{1/2}\,\text{eV}. \tag{15}$$

In principle, one could expect much more significant broadening due to the macroscopic motions. But if plasma in the shell is threaded by magnetic field lines (which I consider to be the most likely possibility), then the maximum gradient of the macroscopic velocity V_m that we can adopt is of the order of the gravitational potential gradient. Taking into account that in all cases of practical interest $\delta \ll r_A$, we can get

$$\Delta\epsilon_m \approx \epsilon\frac{\Delta V_m}{c} \approx \epsilon\frac{\delta}{2r_A}\frac{0.3\,v_{ff}}{c} = 4.3\times10^{-4}\xi R_6\Omega_s^{-1}\left(\frac{M_\odot}{M}\right)\text{eV}. \tag{16}$$

Due to the small profile width (**15**) and (**16**), the Alfvén shell at each point is optically thick for the line photons. The detailed analysis[30] shows, however, that the processes of "true absorption" are not effective enough to prevent their escape from the shell.

To a distant observer the iron line will have a much broader profile due to the Compton scattering and superposition of macroscopic velocities from different parts of the Alfvén shell. Since the Thomson optical thickness of the shell $\tau_T \approx 0.5$–1 (see Equation 4), while the optical depth with respect to the resonance scattering greatly exceeds 1, every line photon undergoes at least one scattering by an electron. After the very first such scattering a photon with the energy $\epsilon = 6.7$ keV spreads due to the Doppler effect over the energy interval[31]

$$\Delta\epsilon = \epsilon(4kT/m_eC^2)^{1/2} \approx 180\,T_6^{1/2}\,\text{eV} \tag{17}$$

and comes out of resonance. The Compton recoil has the same order of magnitude,

$$\Delta\epsilon \approx -\epsilon^2/m_eC^2 \approx -90\,\text{eV}. \tag{18}$$

The flow of gas along the Alfvén surface broadens the line profile by

$$\Delta\epsilon \sim \epsilon\frac{0.3\,V_{ff}}{C} \approx 110\,r_8^{-1/2}(M/M_\odot)^{1/2}\,\text{eV}. \tag{19}$$

Thus, *the observed line profile should have FWHM ~ 200–400 eV.* At such width different transitions in one and the same ion blend, and one might hope to resolve the observed iron line in no more than two components corresponding to ions Fe^{+25} and Fe^{+24}.

A salient feature of the line emission mechanism under discussion is that the line photons are created at the expense of photons from the ionizing continuum. To the corresponding suppression of continuum one must add the emission resulting from direct recombinations to the ground state. FIGURE 2 illustrates the shape of the x-ray

spectrum in the 6–10-keV region that one could expect from Her X-1 for $r_8 = 0.2$ and $\mu_{30} = 1$. The spectrum is averaged over all sight directions. In evaluating the line profile, only the Doppler broadening by scattering on thermal electrons was accounted for. Note that the Fe^{+25} emission comprising some 6% of the total equivalent width is absolutely undistinguishable against the Fe^{+25} line.

In reality, the recombination line of Fe^{+24} should be much less conspicuous than in FIGURE 2 because of (i) the reduction of Fe^{+25} abundance after Fe^{+23} and other lower ions of iron are included into the ionization equilibrium, and (ii) smearing effect of Compton scattering and macroscopic motions not accounted for in FIGURE 2. A small (~10%) decrease of the continuum level at $\epsilon \gtrsim 9$ keV predicted in this model is unlikely to be detected with proportional counters, but must be discovered of course

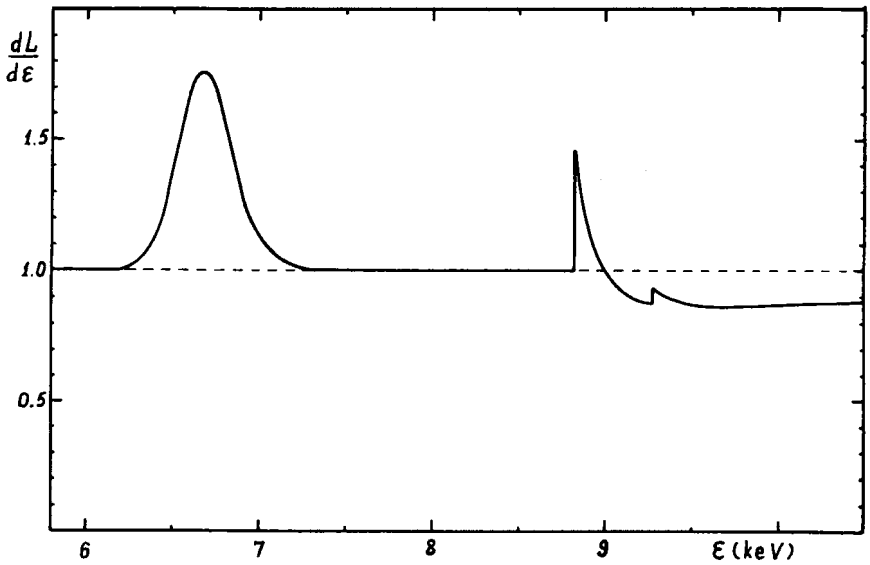

FIGURE 2. The approximate shape of the x-ray spectrum in the vicinity of the iron line that one would expect from Her X-1 for $r_A \approx 2 \times 10^7$ cm and $\mu = 10^{30}$ G cm^3. The spectrum is averaged over a period of 1.24-s pulsations.

with more sensitive spectral instruments. If shielding by the Alfvén shell is the principal cause of pulsing behavior of Her X-1[21,22] then the *K*-edge absorption at $\epsilon \geq 8.83$ keV should be most pronounced between the pulses and may amount to ~30–40% there.

SOFT X-RAY EMISSION

The plasma in the Alfvén shell has been already proposed[21–23] as the most likely source of the strong emission in a soft x-ray band $\epsilon = 0.1$–0.5 keV discovered in Her

X-1.[32] The results of the line emission calculations have some important implications for such an interpretation.

If one demands that, in accordance with observations, the equivalent width of the iron line emitted by the Alfvén shell in Her X-1 be $W \approx 200$–300 eV, then, as calculated above, the plasma temperature in the shell $T \approx 10^6$ K, while its optical thickness for free–free absorption at $\epsilon \lesssim kT$ is greater than 1. This implies that the spectrum of the bremsstrahlung from the shell must be close to that of a blackbody with temperature $T \approx 10^6$ K, which is in excellent agreement with the observations.[32] But the radius of the Alfvén shell r_A in this case turns out to be significantly (by an order of magnitude) less than the conventional value $r_A \approx r_A^0$ (see Equation 1), which results in a rather low value of the total soft x-ray luminosity L_{ff}; see TABLES 1 and 2. The ratios $L_{ff}/L \lesssim 0.02$–0.03, predicted by the present model, are at least an order of magnitude too small to match the observations of Her X-1.[32] From the point of view of this model, the contradiction can be resolved either if an interstellar extinction is overestimated in reference 32, or if there is some other soft x-ray source, much more powerful than the Alfvén shell, in the HZ Her/Her X-1 system.

If the Alfvén shell, corotating with the neutron star, is the principal source of soft x-rays, then the following observational test can be proposed: the 1.24-s pulsations in soft x-rays must correlate in phase with the pulsations of the *absolute* energy flux in the line—the maximum of the soft x-ray flux should always correspond to the maximum flux in the line.

IRON LINE EMISSION IN OTHER X-RAY BINARIES

If one assumes that the model under consideration is general enough and can be applied to the whole class of binary x-ray sources, then immediately a conclusion suggests itself that strong iron line emission is to be found in the spectra of pulsating sources only, since it is x-ray pulsars that possess strong magnetic fields necessary for the existence of the Alfvén shell. To this one must add an empirical fact that the pulsating sources usually have harder x-ray continua, which is not the least important for high values of the equivalent width. And though the observational data, published up to now, are rather scarce, the above conclusion seems to agree with them. Among the best studied x-ray binaries a strong iron line has been detected in the spectra of Her X-1,[3] Cen X-3,[33] and 4U090040040,[5] well known x-ray pulsars, while all the efforts to find this line in the spectra of the much brighter sources, Sco X-1 and Cyg X-1,[34] which do not pulsate, have been unsuccessful.

Special attention should be paid to the x-ray source Cyg X-3, which produces the most powerful iron line emission of all x-ray binaries, $W \approx 1$–2 keV.[2,6] This source has not yet proven to be an x-ray pulsar of the same type as Her X-1 and Cen X-3. Only one period, $p = 4.8^h$, has been firmly established in its flux variations, which may conceivably represent the orbital motion as well as the spinning of the neutron star.[35] Below I show that the above model can be applied to this x-ray source too, without leading to any obvious contradiction with the observations.

The principle mechanism of line excitation in the above model is fluorescence, which, due to a high density of the ionizing x-ray flux, occurs at the frequency $\epsilon = 6.7$–6.9 keV, as contrasted to the fluorescence of cold iron $\epsilon = 6.40$ keV.[19] There are

two observational evidences that favor such an interpretation: (i) the photon energy in the line as measured with the crystal spectrometer[7] is $\epsilon = 6.84 \pm 0.17$ keV, and (ii) the absolute energy flux in the line seems to remain constant[36] when Cyg X-3 undergoes transitions from a low to the high state, and the x-ray flux at $\epsilon \sim 4$ keV increases by an order of magnitude.[2] The latter property becomes a natural consequence of the fluorescence mechanism, if one notes that the x-ray flux at $\epsilon > 8.8$ keV, responsible for the line excitation, does not show any noticeable change in such transitions.[2] Relatively large values of the equivalent width, $W \gtrsim$ keV, can be explained in terms of large x-ray luminosity (cf. Equation 14)—even in the low state $L > 4 \times 10^{37}$ $(d/10$ kpc$)^2$ erg s^{-1}.[2] As for the shift of the line center from 6.7 to 6.5 keV with the binary phase,[6] one apparently has to construct a more detailed model of Cyg X-3 to account for this effect.

Main Conclusions

The above calculations convince us that in principle the powerful iron line emission, discovered in the spectra of several x-ray binaries, can be interpreted as the reradiation of the x-ray continuum, emerging from the surface of the neutron star, by the plasma shell on the Alfvén surface. If one requires $W \approx 300$ eV in the case of Her X-1, then for $n_{Fe} = 3 \times 10^{-5} n_H$, $\mu = 10^{30}$ G cm^3, and $L = 3 \times 10^{37}$ erg s^{-1} one arrives at the following values of the shell parameters: $r_A \approx 2 \times 10^7$ cm $\approx 0.1\ r_A^0$, $n_e \approx 3 \times 10^{20}$ cm^{-3}, and $T \approx 1.5 \times 10^6$ K. The most striking is an unusually low value of the Alfvén radius r_A, which is in conflict with theoretical estimates[28] and too small to account for the observed soft x-ray flux.[32] In view of this, any observational test that could support or refute the above model becomes of special interest.

The model presented here predicts an appreciable spectral width of the observed iron line, $\epsilon/\Delta\epsilon \lesssim 15$–$30$, centered at the energy $\epsilon = 6.70$ keV ($2^3P_1 \rightarrow 1^1S_0$ transition in heliumlike iron), which makes it clearly distinct from the K_α emission of low ionized iron with $\epsilon = 6.40$ keV and $\epsilon/\Delta\epsilon \sim 200$–$300$. The latter result implies that, in order to obtain the shape of the iron line profile in x-ray binaries, one does not necessarily have to build detectors with a very high spectral resolution $\epsilon/\Delta\epsilon \sim 10^3$–$10^4$.

References

1. Sanford, P. W., K. O. Mason & J. Ives. 1975. Mon. Not. R. Astron. Soc. **173:** 9P.
2. Serlemitsos, P. J., E. A. Boldt, S. S. Holt, R. E. Rothschild & J. L. R. Saba. 1975. Astrophys. J. Lett. **201:** L9.
3. Pravdo, S. H., R. H. Becker, E. A. Boldt, S. S. Holt, P. J. Serlemitsos & J. H. Swank. 1977. Astrophys. J. Lett. **215:** L61.
4. Pravdo, S. H., E. A. Boldt, S. S. Holt & P. J. Serlemitsos. 1977. Astrophys. J. Lett. **216:** L23.
5. Becker, R. H., R. E. Rothschild, E. A. Boldt, S. S. Holt, S. H. Pravdo, P. J. Serlemitsos & J. H. Swank. 1978. Astrophys. J. **221:** 912.
6. Becker, R. H., J. K. Robinson-Saba, E. A. Boldt, S. S. Holt, S. H. Pravdo, P. J. Serlemitsos & J. H. Swank. 1978. Astrophys. J. Lett. **224:** L113.
7. Kestenbaum, H. L., K. S. Long, R. Novick, M. C. Weisskopf & R. S. Wolff. 1977. Astrophys. J. Lett. **216:** L19.

8. SERLEMITSOS, P. J., E. A. BOLDT, S. S. HOLT, R. RAMATY & A. F. BRISKEN. 1973. Astrophys. J. Lett. **184:** L1.
9. DAVISON, P. J. N., J. L. CULHANE & R. J. MITCHELL. 1976. Astrophys. J. Lett. **206:** L37.
10. PRAVDO, S. H., R. H. BECKER, E. A. BOLDT, S. S. HOLT, R. E. ROTHSCHILD, P. J. SERLEMITSOS & J. H. SWANK, 1976. Astrophys. J. Lett. **206:** L41.
11. BECKER, R. H., E. A. BOLDT, S. S. HOLT, S. H. PRAVDO, R. E. ROTHSCHILD, P. J. SERLEMITSOS & J. H. SWANK. 1976. Astrophys. J. Lett. **209:** L65.
12. MUSHOTZKY, R. F., P. J. SERLEMITSOS, R. H. BECKER, E. A. BOLDT & S. S. HOLT. 1978. Astrophys. J. **220:** 790.
13. MITCHELL, R. J., J. L. CULHANE, P. J. N. DAVISON & J. C. IVES. 1976. Mon. Not. R. Astron. Soc. **175:** 29.
14. SERLEMITSOS, P. J., B. W. SMITH, E. A. BOLDT. S. S. HOLT & J. H. SWANK, 1977. Astrophys. J. Lett. **211:** L63.
15. MUSHOTZKY, R. F., P. J. SERLEMITSOS, B. W. SMITH, E. A. BOLDT & S. S. HOLT. 1978. Astrophys. J. **225:** 21.
16. MESZAROS, P. 1974. Astron. Astrophys. **35:** 171.
17. BASKO, M. M., R. A. SUNYAEV & L. G. TITARCHUK. 1974. Astron. Astrophys. **31:** 249.
18. HATCHETT, S. & R. WEAVER. 1977. Astrophys. J. **215:** 285.
19. BASKO, M. M. 1978. Astrophys. J. **223:** 268.
20. PRAVDO, S. H., E. A. BOLDT, S. S. HOLT, R. E. ROTHSCHILD & P. J. SERLEMITSOS. 1978. Astrophys. J. **225:** L53.
21. MCCRAY, R. & F. K. LAMB. 1976. Astrophys. J. Lett. **204:** L115.
22. BASKO, M. M. & R. A. SUNYAEV. 1976. Astron. Zh. **53:** 950.
23. SUNYAEV, R. A., 1976. Pisma Astron. Zh. **2:** 287.
24. ARONS, J. & S. M. LEA. 1976. Astrophys. J. **207:** 914.
25. ELSNER, R. F. & F. K. LAMB. 1977. Astrophys. J. **215:** 897.
26. BASKO, M. M. 1977. Astron. Zh. **54:** 1051.
27. SCHARLEMANN, E. 1978. Astrophys. J. **219:** 617.
28. GHOSH, P. & F. K. LAMB. 1978. Astrophys. J. Lett. **223:** L83.
29. BUFF, J. & R. MCCRAY. 1974. Astrophys. J. **189:** 147.
30. BASKO, M. M. 1978. Preprint of Space Research Institute No. 450.
31. CHANDRASEKHAR, S. 1960. Radiative Transfer. Dover, New York.
32. SHULMAN, S., H. FRIEDMAN, G. FRITZ, R. C. HENRY & D. J. YENTIS. 1975. Astrophys. J. Lett. **199:** L101.
33. SWANK, J. H. 1977. Private communication.
34. BOLDT, E. A. 1977. Ann. N.Y. Acad. Sci. **302:** 329.
35. SUNYAEV, R. A. 1976. Pisma Astron. Zh. **2:** 334.
36. PRAVDO, S. H. 1978. Preprint.